

SPECIAL ISSUE

High Resolution Rovibrational and Rotational Spectroscopy of H_2CCCH^+

Wesley Guilherme Dias de Paiva Silva^a, Divita Gupta^a, Eline Plaar^a, José Luis Doménech^b, Stephan Schlemmer^a, Oskar Asvany^a

^a I. Physikalisches Institut, Universität zu Köln, Zùlpicher Str. 77, 50937 Köln, Germany;

^b Instituto de Estructura de la Materia, IEM-CSIC, Serrano 123, 28006 Madrid, Spain

ARTICLE HISTORY

Compiled February 2, 2024

ABSTRACT

The rovibrational spectrum of the molecular ion H_2CCCH^+ was investigated in a 4 K cryogenic ion trap instrument employing the leak-out spectroscopy method. Transitions within the fundamental ν_1 (C-H stretch) and the combination band $\nu_3+\nu_5$ (C-C stretches) were detected, the search aided by high level quantum chemical calculations. The analysis of the rovibrational measurements enabled us to predict the rotational structure of the ground state. Using a rotational-vibrational double-resonance scheme, 14 pure rotational transitions were measured. This, in turn, led to the radio astronomical detection of H_2CCCH^+ in the interstellar medium, as recently reported (Silva et al., *Astron. Astrophys.* 676, L1, 2023).

KEYWORDS

ion traps; rovibrational spectroscopy; rotational spectroscopy; molecular cations

1. Introduction

Astrochemical models (see, e.g., [1]) show that C_3H_3^+ cations play an important role in the chemical evolution of the interstellar medium (ISM). They are considered to undergo dissociative recombination with electrons, leading to the formation of neutral C_3H_2 and C_3H , which are well known molecules in space [2, 3, 4, 5]. The two most stable isomers of C_3H_3^+ are the cyclopropenyl (*c*- C_3H_3^+ , D_{3h}) and the open chain propargyl (H_2CCCH^+ , C_{2v}) cation. Although H_2CCCH^+ is 27.9 kcal/mol less stable than *c*- C_3H_3^+ [6], spectroscopic signals from both isomers have been previously observed in the laboratory, and also, both are predicted to exist in space.

Initial reports on C_3H_3^+ focused on its structural characterization by infrared (IR) spectroscopy in neon matrices and solutions of salts [7, 8]. Later, the gas-phase IR photodissociation (IRPD) spectra of weakly bound complexes of C_3H_3^+ with several tags, including Ne, Ar, H_2 , O_2 , N_2 and CO_2 have been reported both experimentally and theoretically [9, 10, 11, 12, 13, 14, 15]. Additional knowledge on the isomers of C_3H_3^+ comes from photoelectron [16, 17] and electronic [17] spectroscopic studies. While the vibrational frequencies obtained from IRPD spectra of such complexes provide useful structural information, astronomical identification often requires high resolution studies of the bare species. Such information was first provided by Zhao

et al. [18], who investigated the rovibrational spectrum of the ν_4 antisymmetric C-H stretch of $c\text{-C}_3\text{H}_3^+$. Their spectral identification was supported by high level quantum chemical calculations [6, 19]. But due to the absence of a permanent dipole moment in $c\text{-C}_3\text{H}_3^+$, its detection by radio astronomy is prohibited.

With an eye on a potential radio astronomical detection, we investigated those isomers and isotopologues of C_3H_3^+ which possess a permanent dipole moment, and studied the rovibrational and rotational spectra of the singly deuterated $c\text{-C}_3\text{H}_2\text{D}^+$ [20] and the open chain H_2CCCH^+ cation. These investigations culminated in the detection of H_2CCCH^+ in the cold molecular cloud TMC-1, whereas only upper limits could be given for the column density of $c\text{-C}_3\text{H}_2\text{D}^+$ in the same source [21]. In this work, we would like to give a thorough account on the rovibrational spectroscopy of H_2CCCH^+ , for which the ν_1 and $\nu_3+\nu_5$ bands have been measured in high resolution. A brief description of the double resonance scheme, which enabled the measurement of pure rotational lines, is also given here.

2. Experimental

The rovibrational spectrum of H_2CCCH^+ was recorded in the 4 K 22-pole ion trap instrument COLTRAP, which has been described in detail previously [22, 23]. The H_2CCCH^+ ions were created in a storage ion source (SIS) via electron impact ionization ($E_e \approx 25 - 30$ eV) of the precursor gas allene (C_3H_4), which was admitted to the source at a pressure of about 10^{-5} mbar. The created ions were then extracted from the source, mass selected in a first mass filter for mass 39 u, which corresponds to all possible isomers of C_3H_3^+ produced in the SIS and other possible species with the same mass, and injected into the trap. The trap is mounted on a Sumitomo cold head and maintains an ambient temperature of 4 K. To ensure thermalization of the ions to the cryogenic temperature, the trap is constantly filled with He buffer gas ($n \approx 10^{13}$ cm^{-3}).

Once trapped, the rovibrational transitions of H_2CCCH^+ were measured using the novel leak-out spectroscopy (LOS) method [24]. LOS is a universal action spectroscopic approach, which is based on the escape of ions from the trap due to collision-induced transfer of (a fraction of) the ion's internal energy into kinetic energy. Specifically, after the ions are loaded into the trap, they are cooled for 40 ms via collisions with He, after which they are irradiated for 500 ms by an IR beam traversing the trap. In the case of resonance, the ions are elevated into vibrationally excited states. These vibrationally excited ions can then collide with noble gas atoms present in the trap. We used here Ne as the collision partner and it was pulsed additionally into the trap as a 1:3 Ne:He mixture via a piezoelectrically actuated valve. When an ion encounters a Ne atom in the trap, a substantial part of the vibrational energy can be transferred into kinetic energy of the colliding pair. With a neutral-to-ion mass ratio of 20:39 a maximum kinetic energy of $[20/(20 + 39)] \cdot 3200 \text{ cm}^{-1} = 1085 \text{ cm}^{-1} \approx 0.13 \text{ eV}$ can be gained by the ion. By keeping the electrostatic potential barrier at the exit electrode of the trap below 130 mV, fast H_2CCCH^+ ions may leak out from the trap. These escaping ions are then mass selected in a second mass filter, and counted in an ion detector. By repeating these trapping cycles at a rate of 1 Hz, and counting the escaping ions as a function of the laser wavenumber, the rovibrational spectrum of H_2CCCH^+ is recorded.

The IR beam was supplied by a continuous wave optical parametric oscillator (cw-OPO, Aculight Argos Model 2400, Module C) operating in the $3 \mu\text{m}$ spectral

region. The beam entered the vacuum environment through a diamond window (0.6 mm thickness, Diamond Materials GmbH), irradiated the ions by crossing the 22-pole trap, and exited the instrument via a CaF₂ window, after which it was absorbed by a power meter. The measured power was on the order of a few hundred mW. The frequency of the IR radiation was measured by a Bristol wavemeter (Model 621A), which has an accuracy of about 0.001 cm⁻¹.

The pure rotational transitions of H₂CCCH⁺ are recorded by using a double-resonance spectroscopy scheme based on LOS [25]. For this, the IR beam is overlapped with a mm-wave beam outside the apparatus, and both steered into the 22-pole trap simultaneously. The diamond window mentioned above guarantees transparency for both frequency regimes. The mm-wave radiation is produced by a microwave synthesizer (Rohde & Schwarz SMF 100A) that drives an amplifier/multiplier chain source (Virginia Diodes Inc. or Radiometer Physics GmbH). The synthesizer is locked to a Rb atomic clock with a typical stability of 10⁻¹¹.

3. Results

3.1. Identification of carrier of spectroscopic signal

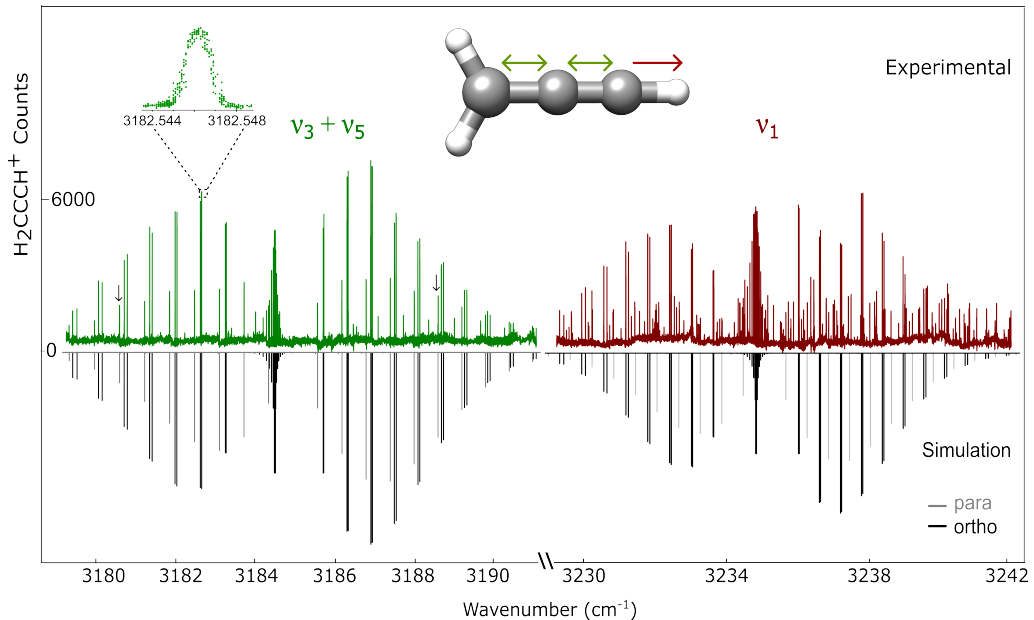


Figure 1. Rovibrational spectra of the $\nu_3 + \nu_5$ (3184.915 cm⁻¹, green) and ν_1 (3235.334 cm⁻¹, red) bands of H₂CCCH⁺ recorded using the novel LOS method. The top portion shows the experimental spectra, while the simulated spectra are given at the bottom. The simulations are obtained at a rotational temperature of $T_{rot} = 10$ K, using the final fitted parameters given in Table 1. In the simulations, the para ($K_a = 0$) and ortho ($K_a = 1$) transitions are distinguished by the gray and black colours, respectively, with an ortho-para ratio of 3:1. The inset shows the rovibrational line $2_{12} \leftarrow 3_{13}$ in the $\nu_3 + \nu_5$ band. With a FWHM of 42 MHz, the kinetic temperature of the ions is estimated as $T_{kin} = 15$ K.

H₂CCCH⁺ is a closed-shell molecule of point group symmetry C_{2v} with an electronic ground state of 1A_1 . It is a near-prolate asymmetric top with an asymmetry parameter $\kappa = -0.9976$, calculated from the rotational constants given by Huang et al.[6].

The rotationally resolved spectra of the ν_1 and $\nu_3 + \nu_5$ parallel bands (both a_1 symmetry) are depicted in Fig. 1 in red and green traces, respectively. A simulation of the spectral features using the PGOPHER program [26] is also provided as black and gray sticks in Fig. 1 for illustration. The identification of these features as being the ν_1 acetylenic C-H stretch and the $\nu_3 + \nu_5$ combination band of both C-C stretches is supported by high level quantum chemical calculations [6] and earlier observations from IRPD experiments [15]. Also, based on these works, we exclude fundamental or combination/overtone bands of $c\text{-C}_3\text{H}_3^+$ to be responsible for the observed spectral features. Specifically, measurements of these particular bands from Ne-tagging experiments [9] locate the $\nu_3 + \nu_5$ band at 3184 cm^{-1} and the ν_1 band at 3238 cm^{-1} . The latter is the assignment given later by Botschwina et al. [12]. Ar-tagging experiments [27] observe the $\nu_3 + \nu_5$ band at 3182 cm^{-1} , also re-assigned by Botschwina et al. [12], and the ν_1 band at 3238 cm^{-1} . These assignments are also in agreement with the high level *ab initio* calculations from Huang et al. [6], namely $\nu_3 + \nu_5$ and ν_1 at 3193 and 3228 cm^{-1} , respectively. In a more recent Ne-tagging experiment, Marimuthu et al. [15] calculate the ν_1 band to be at 3230 cm^{-1} , but neither ν_1 nor $\nu_3 + \nu_5$ were observed in their Ne- C_3H_3^+ IRPD spectrum (see their Fig. 4).

3.2. Spectral Analysis

With the lines of both bands in Fig. 1 being a -type transitions (i.e. $\Delta K_a = 0$, $\Delta K_c = \pm 1$), we anticipated observing transitions with $K_a = 1 \leftarrow 1$ and $K_a = 0 \leftarrow 0$, whereas transitions with $K_a \geq 2$ were not expected due to the large A rotational constant of H_2CCCH^+ and the low temperature conditions in the trap. The most dominant features in the spectra were the series of $K_a = 1 \leftarrow 1$ doublets, which were readily identified in both bands reported here. Preliminary fits of the rotational constants B and C from these observations agreed well with those predicted by high level *ab initio* calculations [6], confirming further the unequivocal detection of H_2CCCH^+ . Although peaks with $K_a = 0 \leftarrow 0$ were expected to be relatively intense, it was very challenging to identify these transitions in the ν_1 band because these lines (i) turned out to be somewhat weaker (please see Fig. 1 and discussion in Section 4), (ii) exhibited perturbations, (iii) were embedded in a plethora of unidentified spectral features (Fig. 1), and, in hindsight, (iv) the calculated A_1 rotational constant (i.e., the rotation-vibration interaction term α_1^A) turned out to be misleading in sign and magnitude, see Table 1.

Fortunately, the combination band $\nu_3 + \nu_5$ contained only few unidentified lines, and exhibited only small perturbations, allowing the $K_a = 0 \leftarrow 0$ transitions to be readily identified. The assignment of the $K_a = 0 \leftarrow 0$ subband within $\nu_3 + \nu_5$ was helped by a small perturbation in the upper $J_{K_a K_c} = 6_{06}$ quantum level, leading to a splitting of 0.064 cm^{-1} which could be spotted in the corresponding transitions in the P- and R-branches and are indicated by small arrows in Fig. 1. The split lines are also given in the line lists in the supplementary material. These assignments allowed first measurements of pure rotational lines with $K_a = 0 \leftarrow 0$ using double resonance spectroscopy, as outlined in the following section, and thus a complete determination of the ground vibrational state of H_2CCCH^+ was obtained.

Due to the difficulties mentioned above, the search for the $K_a = 0 \leftarrow 0$ subband of ν_1 was more challenging. To identify these transitions, we used our knowledge gained of the ground state rotational structure, and compared it to combination differences (CDs, see, e.g., references [28, 29, 30]) formed blindly in the ν_1 state. First, we removed all assigned $K_a = 1 \leftarrow 1$ transitions from the ν_1 spectrum and formed all possible

CDs with the remaining lines. With about $N = 130$ unassigned lines, we obtained $N(N - 1)/2 = 8385$ CDs. This list of CDs must contain those of the ground state, the so-called GSCDs, with $K_a = 0$. From our mm-wave measurements, these GSCDs are constrained to kHz accuracy. Based on this knowledge, one can select pairs of lines from all possible CDs, one in the P-branch and one in the R-branch, namely $P(J + 2)$ and $R(J)$, which are connected by a common rotational quantum level $J + 1$ in the upper ν_1 state and form the GSCD $\approx B_0(4J + 6)$. These pairs of lines with the proper GSCD are then potential members of the $K_a = 0 \leftarrow 0$ subband. This approach is illustrated by a table of GSCDs in the supplementary material. Our final assignments of the $K_a = 0 \leftarrow 0$ lines in ν_1 were then confirmed also with double resonance spectroscopy measurements, as shown in the following subsection.

A detailed list of all assigned lines within ν_1 and $\nu_3 + \nu_5$ is given in the supplementary material. Overall, the observed rovibrational lines in both bands exhibit narrow Doppler widths, given the low temperature of the ion trap. The line $2_{12} \leftarrow 3_{13}$ in the $\nu_3 + \nu_5$ band depicted in the inset of Fig. 1, for example, has a full width at half maximum (FWHM) of about 42 MHz which corresponds to a kinetic temperature of 15 K. The obtained temperature is slightly higher than the nominal trap temperature due to known heating effects [31].

3.3. Double-resonance rotational measurements

Rotational-vibrational double resonance methods are a superb tool to measure rotational fingerprints of molecular ions investigated in cold ion traps [32]. The particular double resonance approach which involves the LOS action spectroscopic scheme has only recently been developed [25]. The application of this rotational method to H_2CCCH^+ , and in particular the subsequent detection of this ion in the cold molecular cloud TMC-1 have already been documented [21]. In that publication, the 14 laboratory mm-wave transitions as well as ground state rotational and centrifugal parameters are listed for H_2CCCH^+ . Additionally, a summary of all measured rotational transitions as well as a comparison to a simulation is given in Fig. S1 of the supplementary material.

In this paper, we would like to highlight the ability of the double resonance method to establish the connectivity of transitions and thus to confirm assignments. As outlined above, these assignment checks were crucial for the transitions with $K_a = 0 \leftarrow 0$, in particular within the heavily perturbed ν_1 band. As an example, Fig. 2 shows the rotational line $8_{08} \leftarrow 7_{07}$ at 152118.074 MHz, detected with the IR laser fixed at 3230.208 cm^{-1} , the $7_{07} \leftarrow 8_{08}$ transition in the ν_1 band.

3.4. Spectroscopic fits

The spectroscopic constants for the ν_1 and $\nu_3 + \nu_5$ bands were obtained by fitting the assigned lines using a Watson's S-reduced Hamiltonian in the I' representation as implemented in Western's PGOPHER program [26]. In these fits, the values of the ground state rotational and centrifugal distortion constants were kept fixed to those determined from pure rotational transitions due to their higher accuracy [21]. As expected, the ground state parameters of H_2CCCH^+ are very similar to those of its deprotonated counterpart, H_2CCC [33], or those of ketene, H_2CCO [34, 28]. Such molecules are distinguished by their large A rotational and D_K centrifugal parameters. As the centrifugal distortion constants in the vibrationally excited states could not be

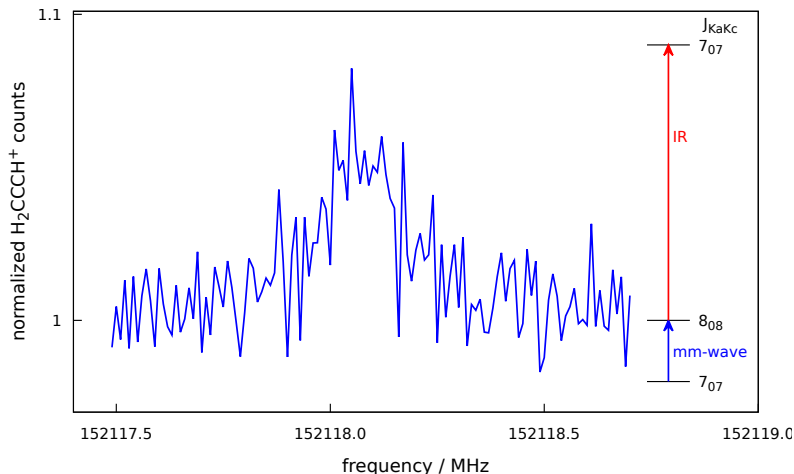


Figure 2. Pure rotational transition $J'_{K_a'K_c'} \leftarrow J''_{K_a''K_c''} = 8_{08} \leftarrow 7_{07}$ (blue trace and blue arrow) of H_2CCCH^+ , recorded using the double resonance spectroscopic scheme. For this measurement, the IR laser frequency (red arrow) was kept fixed on resonance with the ν_1 $7_{07} \leftarrow 8_{08}$ rovibrational transition at 3230.208 cm^{-1} , while the mm-wave frequency was stepped in an up-and-down manner in 10 kHz steps.

well determined, they were also fixed to their ground state values, see Table 1. For the ν_1 band, 54 assigned lines were used in the fit, 49 of which are from the $K_a = 1 \leftarrow 1$ subband. Although many transitions with $K_a = 0 \leftarrow 0$ could be identified in the ν_1 state via combination differences (see the complete line list in the supplementary material), only five were used in the final fit due to strong perturbations (shifts and splittings). For the $\nu_3 + \nu_5$ band, 65 lines were assigned (see supplementary material), of which 62 lines within the $K_a = 0 \leftarrow 0$ and $K_a = 1 \leftarrow 1$ bands were used in the final fit. It is worth noting that to obtain a satisfactory fit of the 62 lines in the $\nu_3 + \nu_5$ band, the D_{JK} constant had to be released and its derived value (18.2(1) MHz) deviates significantly to that of the ground state (0.4388 MHz). Thus, the value of D_{JK} presented here should be taken with caution as this is likely an artefact of the fit most probably related to perturbations in the $K_a = 0 \leftarrow 0$ subband of $\nu_3 + \nu_5$, as exemplified above for the transitions with upper $J_{K_aK_c} = 6_{06}$ quantum numbers. In an alternative fitting procedure, we kept the D_{JK} constant fixed to the ground state value and only included transitions within the $K_a = 0 \leftarrow 0$ subband with $J < 5$. In this fit, a reasonable rms error of the obs-calc values of 0.0019 cm^{-1} was obtained with the $K_a = 0 \leftarrow 0$ lines exhibiting the largest deviations on the order of 0.006 cm^{-1} , in agreement with the observed perturbations. Nevertheless, the fitted parameters of the first fit are reproduced in Table 1 as this allowed the rotational constants and band origin to be derived with smaller uncertainties. In the future, the observation of transitions with $K_a \geq 2$ (e.g. experiments at higher temperatures) will certainly improve the quality of the fit and permit D_{JK} to be better determined within $\nu_3 + \nu_5$.

Overall, the fits for both states presented in Table 1 are quite reasonable with rms errors of the obs-calc values of 0.0004 cm^{-1} and 0.0003 cm^{-1} for ν_1 and $\nu_3 + \nu_5$, respectively. Please note that the fit results may be somewhat optimistic, as many parameters were fixed. For instance, the uncertainties in the values of A_1 and A_{3+5} reflect only that of the fit and do not take into account the large uncertainty of A_0 itself, which is 247 MHz [21]. Future investigations of a b-type perpendicular band of H_2CCCH^+ , e.g. the antisymmetric CH_2 stretch at around 3093 cm^{-1} [27], may help to

Table 1. Spectroscopic parameters of H_2CCCH^+ (Watson’s S-reduced Hamiltonian) obtained by fitting the rovibrational transitions given in the supplementary material, using Western’s PGOPHER program [26]. The uncertainty in the last digits of each parameter is reported in parentheses. The units are MHz, unless otherwise noted.

Parameter	ground		ν_1		$\nu_3 + \nu_5$	
	exp ^a	<i>ab initio</i> ^b	this work	<i>ab initio</i> ^b	this work	<i>ab initio</i> ^b
ν / cm^{-1}		0	3235.3338(2)	3239.0	3184.9154(1)	3201.8
A	281856	281911.9	274403(6)	281933.2	267652(4)	281534.8
B	9675.841	9580.2	9637.9(1)	9554.3	9625.3(1)	9501.2
C	9342.877	9251.9	9325.6(1)	9227.4	9315.1(1)	9175.9
$D_J \times 10^3$	2.942	3	2.942 ^c	-	2.942 ^c	-
D_{JK}	0.4388	0.479	0.4388 ^c	-	18.2(1)	-
D_K	20.678	20.862	20.678 ^c	-	20.678 ^c	-
$d_1 \times 10^3$	-0.121	0	-0.121 ^c	-	-0.121 ^c	-
$d_2 \times 10^3$	-0.051	0	-0.051 ^c	-	-0.051 ^c	-

^a: ground state parameters fixed to those of Silva et al. [21]. D_K and d_2 are calculated.

^b: values from Huang et al. [6]

^c: Fixed to ground state value

constrain A_0 and D_K better. A similar strategy has been followed for ketene, H_2CCO [34], 50 years ago.

4. Discussion and Outlook

The successful measurement of the rovibrational spectrum of the fundamental ν_1 band (C-H stretch) and the combination band $\nu_3 + \nu_5$ (C-C stretches) for the H_2CCCH^+ cation presented here illustrates the broad applicability and remarkable sensitivity of the recently developed LOS method. The rotational-vibrational double resonance method using LOS, recently demonstrated in our group for the HC_3O^+ ion [25], enabled not only pure rotational transitions for H_2CCCH^+ to be obtained but also the perturbed ν_1 band to be deciphered. A search in the cold interstellar cloud TMC-1 finally led to the detection of this ion in space [21]. A similar approach was followed for another member of the C_3H_3^+ family, the singly deuterated c- $\text{C}_3\text{H}_2\text{D}^+$ cation [20], but unfortunately its low dipole moment and low abundance inhibited detection in TMC-1, and only an upper limit for its column density could be given [21]. In the future, we expect that LOS will enable the characterization of more cations in the laboratory, potentially leading to their detection in space by radio astronomy.

While these results are relevant to astronomers, interesting insights into the molecular structure of H_2CCCH^+ upon vibrational excitation are obtained. In particular, the value of the rotational constant A (Table 1) decreases upon excitation into the ν_1 and $\nu_3 + \nu_5$ states, by 2.7 % and 5 %, respectively. This suggests significant structural changes when the terminal C-H or C-C bonds are excited. The experimentally obtained vibration-rotation interaction constants are about $\alpha_1^A = 7486$ MHz and $\alpha_{3+5}^A = 14483$ MHz, respectively. As the backbone of H_2CCCH^+ lies along the a -axis with only the methylene hydrogens pointing away from this axis, the value of A is intimately related to the value of the average $\angle\text{HCH}$ angle. Considering that A is inversely proportional to the moment of inertia component I_a , it becomes

evident that the smaller values of A_1 and A_{3+5} are likely due to the C-H and C-C stretches that move the methylene hydrogens further apart by increasing the $\angle\text{HCH}$ angle when vibrating. This effect is more pronounced in the ν_{3+5} band as the C-C bonds are spatially closer to the CH_2 group. Although the predictions from Huang et al. [6] support the experimental assignments and show overall good agreement with the determined values, the theoretical calculations do not capture well the trend observed for the changes in the values of A upon vibrational excitation, as seen in Table 1. The calculated predictions are $\alpha_1^A = -21.277$ MHz and $\alpha_{3+5}^A = 377.099$ MHz. These discrepancies may be associated with perturbations in H_2CCCH^+ , which are not well described by standard computational methods. Thus, our high-resolution study of H_2CCCH^+ also provides data which can contribute to the improvement and benchmark of theoretical models.

Although H_2CCCH^+ has been well characterized in this work, many open questions remain concerning its rovibrational spectroscopy. The above mentioned perturbations affect both rovibrational bands, but particularly ν_1 exhibits severe line shifts and splittings. Such severe perturbations have also been observed for ketene [34, 35, 28], and traced back to the presence of low-lying vibrational states, whose overtones and combination bands give rise to Fermi and Coriolis interactions [35, 28]. The unusual effective value for D_{JK} determined for $\nu_3 + \nu_5$ is certainly a consequence of this, as well as the intensity pattern observed both for ν_1 and $\nu_3 + \nu_5$. As H_2CCCH^+ contains a plane of symmetry with two equivalent hydrogen atoms, H_2CCCH^+ has two nuclear spin states, ortho (levels with odd values of K_a) and para (levels with even values of K_a) with an expected ortho-para ratio of 3:1. This situation is very similar to, e.g., neutral H_2CCC [5, 33] or the aforementioned ketene, H_2CCO [34, 28]. From the radio astronomical observations of H_2CCCH^+ , in which the para $2_{02}-1_{01}$ and ortho $2_{12}-1_{11}$ and $2_{11}-1_{10}$ transitions were seen [21], a consistent ortho-para ratio of $3.3(\pm 0.6):1$ was derived. In the rovibrational spectra in Fig. 1, however, the $K_a = 0 \leftarrow 0$ para-transitions exhibit somewhat lower than expected intensities. To reproduce the observed IR spectra, an 'artificial' ortho-para ratio of roughly 4:1 would be needed. We can exclude that the unusual ratio is related to the formation processes of H_2CCCH^+ by electron impact ionization of allene (C_3H_4) in our ion source, because essentially the same spectrum was obtained using a HCCD/ CH_4 precursor mixture, see Fig. S3 in the supplementary material. Also, we do not suspect that our novel LOS method to be responsible for this peculiar observation, as experiments with other ions containing two identical protons exhibited the expected nuclear spin statistics, e.g. C_2H_2^+ [36] and $\text{c-C}_3\text{H}_2\text{D}^+$ [20]. The intensities observed in our spectrum, however, depend on multiple factors like the transition dipole moment, population distribution, trap time, and more. So, to determine an accurate ortho-para population ratio of H_2CCCH^+ in the ion trap all ortho (or para) species shall be leaked out from the trap and the remaining para (or ortho) fraction shall be measured. This new method of determining the nuclear-spin composition in a trap¹ is currently tested in our laboratory for a number of simple cases. Results from these measurements will be published separately. In addition, we plan to perform rovibrational spectroscopy of the b-type antisymmetric CH_2 stretch or one of the fundamental a-type C-C stretches [37] of H_2CCCH^+ . Measurements at higher trap temperature to populate the $K_a = 2$ states or the rovibrational measurement of the perdeuterated version, D_2CCCD^+ , are also in reach.

¹Patent pending: DE 10 2021 127 556.3 (Universität zu Köln), 22.10.2021

5. Acknowledgements

The authors want to dedicate this contribution to Prof. Attila Császár on the occasion of his 60th birthday. The authors also want to thank Xinchuan Huang for reading the manuscript prior to submission. This work has been supported by an ERC advanced grant (MissIons: 101020583) and via Collaborative Research Centre 1601 (project ID: 500700252, sub-project C4) funded by the Deutsche Forschungsgemeinschaft (DFG) and DFG SCHL 341/15-1 (“Cologne Center for Terahertz Spectroscopy”). W.G.D.P.S. thanks the Alexander von Humboldt Foundation for support through a postdoctoral fellowship. J.L.D. acknowledges the support from the MCINN project PID2020-113084GB-I00/AEI/10.13039/501100011033 and the CSIC project ILINK+ LINKA20353.

References

- [1] O. Sipilä, S. Spezzano and P. Caselli, *Astron. Astrophys.* **591**, L1 (2016).
- [2] P. Thaddeus, C.A. Gottlieb, A. Hjalmarson, L.E.B. Johansson, W.M. Irvine, P. Friberg and R.A. Linke, *Astrophys. J. Lett.* **294**, L49–L53 (1985).
- [3] P. Thaddeus, J.M. Vrtilik and C.A. Gottlieb, *Astrophys. J. Lett.* **299**, L63–L66 (1985).
- [4] S. Yamamoto, S. Saito, M. Ohishi, H. Suzuki, S.I. Ishikawa, N. Kaifu and A. Murakami, *Astrophys. J. Lett.* **322**, L55 (1987).
- [5] J. Cernicharo, C.A. Gottlieb, M. Guelin, T.C. Killian, G. Paubert, P. Thaddeus and J.M. Vrtilik, *Astrophys. J. Lett.* **368**, L39 (1991).
- [6] X. Huang, P.R. Taylor and T.J. Lee, *J. Phys. Chem. A* **115** (19), 5005–5016 (2011).
- [7] M. Wyss, E. Riaplov and J.P. Maier, *J. Chem. Phys.* **114**, 10355–10361 (2001).
- [8] N.C. Craig, J. Pranata, S.J. Reinganum, J.R. Sprague and P.S. Stevens, *J. Am. Chem. Soc.* **108**, 4378–4386 (1986).
- [9] D. Roth and O. Dopfer, *Phys. Chem. Chem. Phys.* **4**, 4855–4865 (2002).
- [10] O. Dopfer, D. Roth and J.P. Maier, *J. Am. Chem. Soc.* **124**, 494–502 (2002).
- [11] O. Dopfer, D. Roth and J.P. Maier, *Int. J. Mass Spectrom.* **218** (3), 281–297 (2002).
- [12] P. Botschwina, R. Oswald and O. Dopfer, *Phys. Chem. Chem. Phys.* **13**, 14163–14175 (2011).
- [13] P. Botschwina, R. Oswald and G. Rauhut, *Phys. Chem. Chem. Phys.* **13**, 7921–7929 (2011).
- [14] P. Botschwina and R. Oswald, *J. Chem. Phys.* **134** (4), 044305 (2011).
- [15] A.N. Marimuthu, D. Sundelin, S. Thorwirth, B. Redlich, W.D. Geppert and S. Brünken, *J. Mol. Spectr.* **374**, 111377 (2020).
- [16] H. Gao, Z. Lu, L. Yang, J. Zhou and C.Y. Ng, *J. Chem. Phys.* **137** (16), 161101 (2012).
- [17] G.A. Garcia, B. Gans, J. Krüger, F. Holzmeier, A. Röder, A. Lopes, C. Fittschen, C. Alcaraz and J.C. Loison, *Phys. Chem. Chem. Phys.* **20**, 8707–8718 (2018).
- [18] D. Zhao, K.D. Doney and H. Linnartz, *Astrophys. J. Lett.* **791** (2), L28 (2014).
- [19] X. Huang and T.J. Lee, *Astrophys. J.* **736** (1), 33 (2011).
- [20] D. Gupta, W.G.D.P. Silva, J.L. Doménech, E. Plaar, S. Thorwirth, S. Schlemmer and O. Asvany, *Faraday Discuss.* **245**, 298–308 (2023).
- [21] W.G.D.P. Silva, J. Cernicharo, S. Schlemmer, N. Marcelino, J.C. Loison, M.

- Agúndez, D. Gupta, V. Wakelam, S. Thorwirth, C. Cabezas, B. Tercero, J.L. Doménech, R. Fuentetaja, W.J. Kim, P. de Vicente and O. Asvany, *Astron. Astrophys.* **676**, L1 (2023).
- [22] O. Asvany, F. Bielau, D. Moratschke, J. Krause and S. Schlemmer, *Rev. Sci. Instr.* **81**, 076102 (2010).
- [23] O. Asvany, S. Brünken, L. Kluge and S. Schlemmer, *Appl. Phys. B* **114** (1-2), 203–211 (2014).
- [24] P.C. Schmid, O. Asvany, T. Salomon, S. Thorwirth and S. Schlemmer, *J. Phys. Chem. A* **126**, 8111 (2022).
- [25] O. Asvany, S. Thorwirth, P.C. Schmid, T. Salomon and S. Schlemmer, *Phys. Chem. Chem. Phys.* **25**, 19740–19749 (2023).
- [26] C.M. Western, *J. Quant. Spectros. Rad. Transfer* **186**, 221 – 242 (2017).
- [27] A.M. Ricks, G.E. Douberly, P.v.R. Schleyer and M.A. Duncan, *J. Chem. Phys.* **132** (5), 051101 (2010).
- [28] J.W.C. Johns, L. Nemes, K.M.T. Yamada, T.Y. Wang, J. Doménech, J. Santos, P. Cancio, D. Bermejo, J. Ortigoso and R. Escribano, *J. Molec. Spectrosc.* **156** (2), 501–503 (1992).
- [29] O. Asvany, K.M.T. Yamada, S. Brünken, A. Potapov and S. Schlemmer, *Science* **347** (6228), 1346–1349 (2015).
- [30] S. Brackertz, S. Schlemmer and O. Asvany, *J. Mol. Spectros.* **342**, 73 – 82 (2017).
- [31] O. Asvany and S. Schlemmer, *Int. J. Mass Spectrom.* **279**, 147–155 (2009).
- [32] O. Asvany and S. Schlemmer, *Phys. Chem. Chem. Phys.* **23**, 26602–26622 (2021).
- [33] J.M. Vrtilik, A. Gottlieb, E.W. Gottlieb, T.C. Killian and P. Thaddeus, *Astrophys. J. Lett.* **364**, L53 (1990).
- [34] J.W.C. Johns, J.M.R. Stone and G. Winnewisser, *J. Molec. Spectrosc.* **42** (3), 523–535 (1972).
- [35] J.L. Duncan, A.M. Ferguson, J. Harper, K.H. Tonge and F. Hegelund, *J. Molec. Spectrosc.* **122** (1), 72–93 (1987).
- [36] S. Schlemmer, E. Plaar, D. Gupta, W.G.D.P. Silva, T. Salomon and O. Asvany, *Mol. Phys.* p. e2241567 (2023).
- [37] M. Bast, J. Böing, T. Salomon, S. Thorwirth, O. Asvany, M. Schäfer and S. Schlemmer, *J. Mol. Spectrosc.* **398**, 111840 (2023).

Supplementary Material: High-Resolution Rovibrational and Rotational Spectroscopy of H_2CCCH^+

Wesley G. D. P. Silva,[†] Divita Gupta,[†] Eline Plaar,[†] José L. Doménech,[‡] Stephan
Schlemmer,^{*,†} and Oskar Asvany^{*,†}

[†]*I. Physikalisches Institut, Universität zu Köln*

Zùlpicher Str. 77, 50937 Köln, Germany

[‡]*Instituto de Estructura de la Materia, IEM-CSIC, Serrano 123, 28006 Madrid, Spain*

E-mail: schlemmer@ph1.uni-koeln.de; asvany@ph1.uni-koeln.de

Calibration measurements

We performed additional calibration measurements with neutral C_2H_2 contained in a gas cell. We measured several lines of C_2H_2 between 3190 and 3240 cm^{-1} whose frequencies are given in the HITRAN database (J. Quant. Spectrosc. Radiat. Transfer, 2022, 266, 107949). Following this procedure, we shifted our data up by 0.007 cm^{-1} . With the calibration, the accuracy of our IR measurements should be on the order of 0.001 cm^{-1} .

Linelist of measured transitions and residuals

Table S1: Frequencies and residuals (in cm^{-1}) of the rovibrational transitions observed for the ν_1 band of H_2CCCH^+ . Lines marked with an asterisk (*) were not included in the fit.

transition	frequency	obs-calc
$8_{17} \leftarrow 9_{18}$	3229.2485	-0.0002
$8_{18} \leftarrow 9_{19}$	3229.3732	-0.0002
$8_{08} \leftarrow 9_{09}$	3229.5255*	
$7_{16} \leftarrow 8_{17}$	3229.9057	-0.0002
$7_{17} \leftarrow 8_{18}$	3230.0136	-0.0004
$7_{07} \leftarrow 8_{08}$	3230.2076	-0.0006
$6_{15} \leftarrow 7_{16}$	3230.5609	-0.0001
$6_{16} \leftarrow 7_{17}$	3230.6527	-0.0005
$6_{06} \leftarrow 7_{07}$	3230.8424*	
$5_{14} \leftarrow 6_{15}$	3231.2139	-0.0000
$5_{15} \leftarrow 6_{16}$	3231.2904	-0.0005
$5_{05} \leftarrow 6_{06}$	3231.4815*	
$4_{13} \leftarrow 5_{14}$	3231.8646	-0.0002
$4_{14} \leftarrow 5_{15}$	3231.9266	-0.0005
$4_{04} \leftarrow 5_{05}$	3232.1126*	
	3232.1915*	
$3_{12} \leftarrow 4_{13}$	3232.5131	-0.0003
$3_{13} \leftarrow 4_{14}$	3232.5615	-0.0004
$3_{03} \leftarrow 4_{04}$	3232.7216*	
	3232.7986*	
$2_{11} \leftarrow 3_{12}$	3233.1592	-0.0006
$2_{12} \leftarrow 3_{13}$	3233.1945	-0.0007
$2_{02} \leftarrow 3_{03}$	3233.4284*	
$1_{10} \leftarrow 2_{11}$	3233.8036	-0.0005
$1_{11} \leftarrow 2_{12}$	3233.8264	-0.0006
$1_{01} \leftarrow 2_{02}$	3234.0636	0.0004
$8_{18} \leftarrow 8_{17}$	3234.6321	-0.0003
$0_{00} \leftarrow 1_{01}$	3234.6988	-0.0006
$7_{17} \leftarrow 7_{16}$	3234.7334	0.0002
$6_{16} \leftarrow 6_{15}$	3234.8214	-0.0001
$5_{15} \leftarrow 5_{14}$	3234.8971	-0.0000
$4_{14} \leftarrow 4_{13}$	3234.9602	0.0001
$3_{13} \leftarrow 3_{12}$	3235.0103	-0.0002

$2_{12} \leftarrow 2_{11}$	3235.0482	-0.0001
$1_{11} \leftarrow 1_{10}$	3235.0734	-0.0002
$1_{10} \leftarrow 1_{11}$	3235.0951	0.0000
$2_{11} \leftarrow 2_{12}$	3235.1129	-0.0000
$3_{12} \leftarrow 3_{13}$	3235.1398	0.0001
$4_{13} \leftarrow 4_{14}$	3235.1756	0.0003
$5_{14} \leftarrow 5_{15}$	3235.2203	0.0004
$6_{15} \leftarrow 6_{16}$	3235.2738	0.0004
$7_{16} \leftarrow 7_{17}$	3235.3362	0.0004
$8_{17} \leftarrow 8_{18}$	3235.4076	0.0004
$1_{01} \leftarrow 0_{00}$	3235.9674	0.0010
$2_{12} \leftarrow 1_{11}$	3236.3393	0.0001
$2_{11} \leftarrow 1_{10}$	3236.3596	0.0001
$2_{02} \leftarrow 1_{01}$	3236.6015*	
$3_{13} \leftarrow 2_{12}$	3236.9639	0.0003
$3_{12} \leftarrow 2_{11}$	3236.9932	0.0004
$3_{03} \leftarrow 2_{02}$	3237.1630*	
	3237.2398*	
$4_{14} \leftarrow 3_{13}$	3237.5868	0.0005
$4_{13} \leftarrow 3_{12}$	3237.6245	0.0006
$4_{04} \leftarrow 3_{03}$	3237.8225*	
	3237.9018*	
$5_{15} \leftarrow 4_{14}$	3238.2081	0.0005
$5_{14} \leftarrow 4_{13}$	3238.2536	0.0008
$5_{05} \leftarrow 4_{04}$	3238.4599*	
$6_{16} \leftarrow 5_{15}$	3238.8275	0.0002
$6_{15} \leftarrow 5_{14}$	3238.8800	0.0005
$6_{06} \leftarrow 5_{05}$	3239.0889*	
$7_{17} \leftarrow 6_{16}$	3239.4456	0.0000
$7_{16} \leftarrow 6_{15}$	3239.5045	0.0004
$7_{07} \leftarrow 6_{06}$	3239.7222	-0.0001
$8_{18} \leftarrow 7_{17}$	3240.0628	0.0005
$8_{17} \leftarrow 7_{16}$	3240.1266	0.0003
$8_{08} \leftarrow 7_{07}$	3240.3082*	
$9_{19} \leftarrow 8_{18}$	3240.6781	0.0007
$9_{18} \leftarrow 8_{17}$	3240.7461	-0.0003
$10_{110} \leftarrow 9_{19}$	3241.2885*	
$10_{19} \leftarrow 9_{18}$	3241.3633	-0.0009
$11_{111} \leftarrow 10_{110}$	3241.9055*	
$11_{110} \leftarrow 10_{19}$	3241.9782*	

Table S2: Rovibrational transition frequencies and residuals of lines observed in ν_{3+5} . Lines marked with an asterisk (*) were not included in the fit.

transition	frequency	obs-calc
$8_{08} \leftarrow 9_{09}$	3179.1134	-0.0000
$7_{16} \leftarrow 8_{17}$	3179.2071	0.0002
$7_{17} \leftarrow 8_{18}$	3179.3170	-0.0001
$7_{07} \leftarrow 8_{08}$	3179.7685	0.0003
$6_{15} \leftarrow 7_{16}$	3179.8762	0.0002
$6_{16} \leftarrow 7_{17}$	3179.9698	0.0001
$6_{06} \leftarrow 7_{07}$	3180.4156*	
	3180.4220*	
$5_{14} \leftarrow 6_{15}$	3180.5410	0.0001
$5_{15} \leftarrow 6_{16}$	3180.6189	0.0000
$5_{05} \leftarrow 6_{06}$	3181.0709	0.0006
$4_{13} \leftarrow 5_{14}$	3181.2018	0.0002
$4_{14} \leftarrow 5_{15}$	3181.2646	-0.0002

$4_{04} \leftarrow 5_{05}$	3181.7181	0.0005
$3_{12} \leftarrow 4_{13}$	3181.8582	0.0000
$3_{13} \leftarrow 4_{14}$	3181.9071	-0.0001
$3_{03} \leftarrow 4_{04}$	3182.3623	-0.0001
$2_{11} \leftarrow 3_{12}$	3182.5108	0.0001
$2_{12} \leftarrow 3_{13}$	3182.5462	-0.0001
$2_{02} \leftarrow 3_{03}$	3183.0044	-0.0001
$1_{10} \leftarrow 2_{11}$	3183.1590	0.0001
$1_{11} \leftarrow 2_{12}$	3183.1820	0.0001
$1_{01} \leftarrow 2_{02}$	3183.6435	-0.0005
$7_{17} \leftarrow 7_{16}$	3184.0358	-0.0005
$6_{16} \leftarrow 6_{15}$	3184.1375	-0.0003
$5_{15} \leftarrow 5_{14}$	3184.2246	-0.0004
$0_{00} \leftarrow 1_{01}$	3184.2802	-0.0009
$4_{14} \leftarrow 4_{13}$	3184.2976	-0.0001
$3_{13} \leftarrow 3_{12}$	3184.3558	-0.0000
$2_{12} \leftarrow 2_{11}$	3184.3993	-0.0000
$1_{11} \leftarrow 1_{10}$	3184.4285	0.0001
$1_{10} \leftarrow 1_{11}$	3184.4499	0.0000
$2_{11} \leftarrow 2_{12}$	3184.4638	0.0001
$3_{12} \leftarrow 3_{13}$	3184.4845	-0.0000
$4_{13} \leftarrow 4_{14}$	3184.5122	0.0000
$5_{14} \leftarrow 5_{15}$	3184.5467	-0.0001
$6_{15} \leftarrow 6_{16}$	3184.5881	-0.0003
$7_{16} \leftarrow 7_{17}$	3184.6366	-0.0003
$1_{01} \leftarrow 0_{00}$	3185.5466	-0.0006
$2_{12} \leftarrow 1_{11}$	3185.6904	0.0001
$2_{11} \leftarrow 1_{10}$	3185.7103	0.0001
$2_{02} \leftarrow 1_{01}$	3186.1764	-0.0000
$3_{13} \leftarrow 2_{12}$	3186.3090	0.0002
$3_{12} \leftarrow 2_{11}$	3186.3377	0.0001
$3_{03} \leftarrow 2_{02}$	3186.8030	0.0001
$4_{14} \leftarrow 3_{13}$	3186.9241	0.0002
$4_{13} \leftarrow 3_{12}$	3186.9609	0.0001
$4_{04} \leftarrow 3_{03}$	3187.4275	0.0007
$5_{15} \leftarrow 4_{14}$	3187.5353	-0.0003
$5_{14} \leftarrow 4_{13}$	3187.5797	-0.0001
$5_{05} \leftarrow 4_{04}$	3188.0487	0.0007
$6_{16} \leftarrow 5_{15}$	3188.1437	-0.0001
$6_{15} \leftarrow 5_{14}$	3188.1943	-0.0002
$6_{06} \leftarrow 5_{05}$	3188.6618*	
	3188.6681*	
$7_{17} \leftarrow 6_{16}$	3188.7487	0.0001
$7_{16} \leftarrow 6_{15}$	3188.8051	0.0001
$7_{07} \leftarrow 6_{06}$	3189.2828	0.0003
$8_{18} \leftarrow 7_{17}$	3189.3499	0.0000
$8_{17} \leftarrow 7_{16}$	3189.4115	0.0001
$8_{08} \leftarrow 7_{07}$	3189.8954	-0.0003
$9_{19} \leftarrow 8_{18}$	3189.9484	0.0006
$9_{18} \leftarrow 8_{17}$	3190.0136	0.0000
$9_{09} \leftarrow 8_{08}$	3190.5054	-0.0008
$10_{110} \leftarrow 9_{19}$	3190.5481*	
$10_{19} \leftarrow 9_{18}$	3190.6114	-0.0001
$11_{110} \leftarrow 10_{19}$	3191.2052	0.0001

Combination differences in the ν_1 $K_a = 0 \leftarrow 0$ subband

As mentioned in the main manuscript, only after measuring and assigning the $K_a = 0 \leftarrow 0$ lines in the $\nu_3 + \nu_5$ band, it was possible to predict and subsequently measure a-type rotational transitions with $K_a = 0 \leftarrow 0$, and thus to fully determine the ground state rotational structure of H_2CCCH^+ . This, in turn, allowed the $K_a = 0 \leftarrow 0$ subband in ν_1 to be identified via ground state combination differences (GSCDs), as shown by the table below.

Table S3: GSCDs within ν_1 $K_a = 0 \leftarrow 0$ and comparison to data determined by mm-wave measurements. All values in cm^{-1} . The GSCDs determined via the IR data ("trans1-trans2") are accurate within 0.001 cm^{-1} , while the values based on rotational spectroscopy ("mm-wave") are accurate within a few kHz.

IR transition2	IR transition1	trans2 - trans1	mm-wave	comment
3235.9674 $1_{01} \leftarrow 0_{00}$	3234.0636 $1_{01} \leftarrow 2_{02}$	1.9038 $2_{02} - 0_{00}$	1.9031750	
3236.6015 $2_{02} \leftarrow 1_{01}$	3233.4284 $2_{02} \leftarrow 3_{03}$	3.1730 $3_{03} - 1_{01}$	3.1719165	
3237.2398 $3_{03} \leftarrow 2_{02}$	3232.7986 $3_{03} \leftarrow 4_{04}$	4.4412 $4_{04} - 2_{02}$	4.4405952	perturbed/split
3237.1630	3232.7216	4.4414		perturbed/split
3237.8225 $4_{04} \leftarrow 3_{03}$	3232.1126 $4_{04} \leftarrow 5_{05}$	5.7099 $5_{05} - 3_{03}$	5.7091859	perturbed/split
3237.9018	3232.1915	5.7103		perturbed/split
3238.4599 $5_{05} \leftarrow 4_{04}$	3231.4815 $5_{05} \leftarrow 6_{06}$	6.9785 $6_{06} - 4_{04}$	6.9776637	
3239.0889 $6_{06} \leftarrow 5_{05}$	3230.8424 $6_{06} \leftarrow 7_{07}$	8.2465 $7_{07} - 5_{05}$	8.2460036	
3239.7222 $7_{07} \leftarrow 6_{06}$	3230.2076 $7_{07} \leftarrow 8_{08}$	9.5147 $8_{08} - 6_{06}$	9.5141806	
3240.3082 $8_{08} \leftarrow 7_{07}$	3229.5255 $8_{08} \leftarrow 9_{09}$	10.7827 $9_{09} - 7_{07}$	10.7821699	

Ground state rotational transitions and energy levels

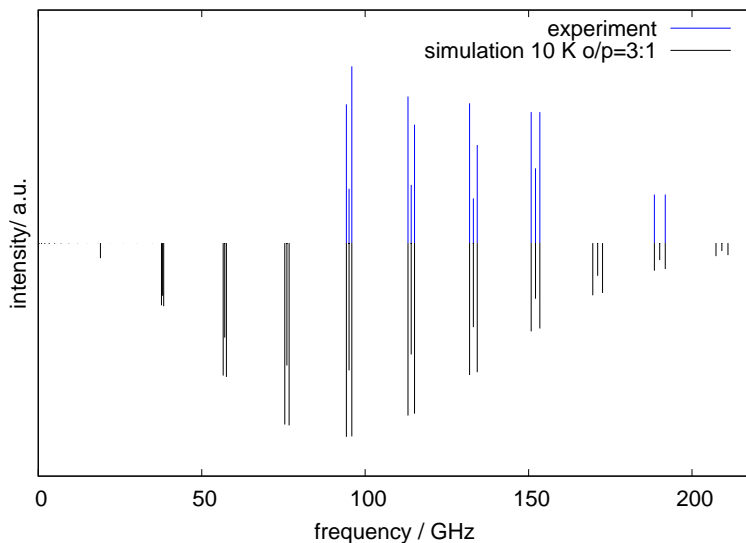


Figure S1: Summary of the 14 rotational lines measured in the course of this project (blue sticks). For the simulation using PGOPHER (black sticks), the ortho and para transitions have been simulated separately at a temperature of 10 K, and then plotted with corresponding weights of 3 and 1, respectively.

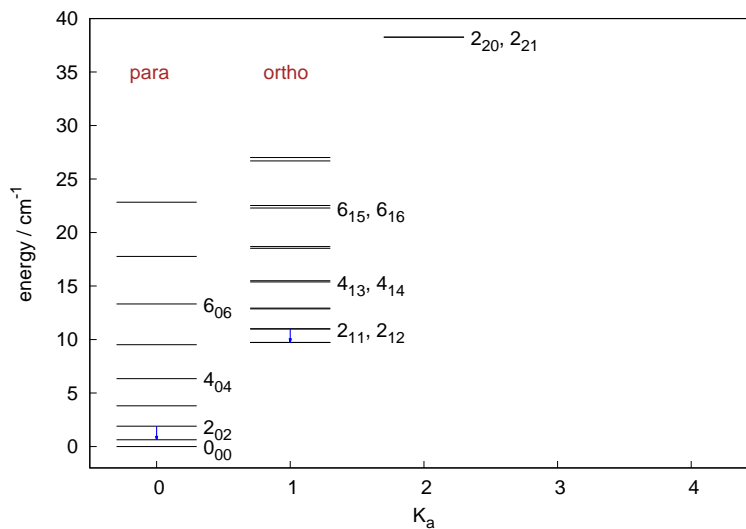


Figure S2: Ground state energy levels of H_2CCCH^+ . In our low-temperature experiment, only para states with $K_a = 0$ and ortho states with $K_a = 1$ are populated.

Comparison of IR spectra from different precursors

Prior to investigating H_2CCCH^+ , we studied in Cologne the IR spectrum of $c\text{-C}_3\text{H}_2\text{D}^+$, produced in the source from the electron impact ionization of a HCCD/CH_4 mixture (Faraday Discuss. 245, 298–308 (2023), doi: 10.1039/d3fd00068k). As the ionization of this mixture also produces substantial amounts of C_3H_3^+ isomers with mass 39 u, our first search for the ν_1 band of H_2CCCH^+ was carried out with this precursor mixture (shown below in red). The observed features were consistent with those predicted for a near prolate asymmetric top, like H_2CCCH^+ . Since our mass selection could also introduce deuterated species with the same mass (39 u) into the trap, we later re-measured the same spectral region using a precursor which does not contain deuterium, and we chose allene (C_3H_4). This measurement corroborated H_2CCCH^+ as the carrier of the spectroscopic signals (shown below in black).

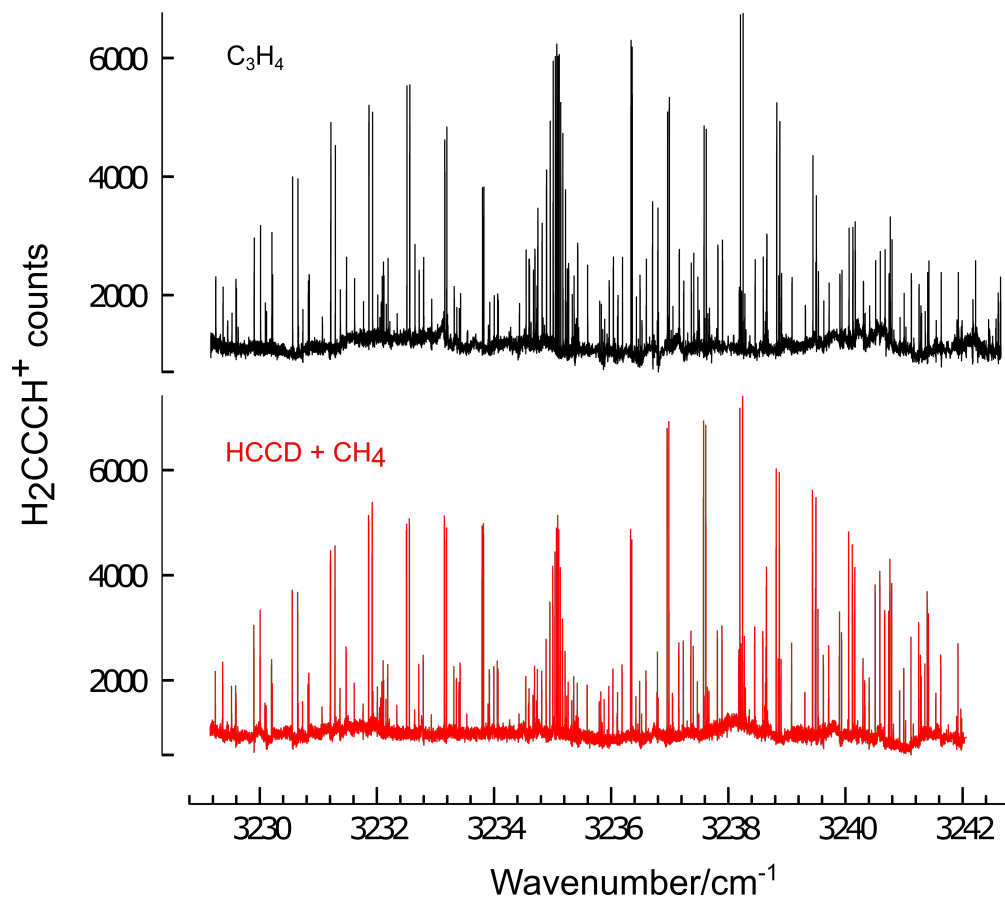


Figure S3: Comparison between the ν_1 band of H_2CCCH^+ recorded with allene C_3H_4 (top, black) and with a mixture of HCCD/CH_4 (bottom, red) as precursors.